

Influence of the discharge circuit inductance on the process of galvanic wastes electrospark purification

Abstract. An effective tool for cleaning galvanic wastes from heavy metal ions is considered - a volumetric-distributed multi-spark submersible discharge. The general patterns of changes in the electrical characteristics of a multi-spark underwater discharge in a layer of a mixture of iron and aluminum granules depending on the inductance of the discharge circuit are revealed. The established patterns make it possible to stabilize the discharge in the course of electrospark treatment of a layer of metal granules in water. The dependences of the power amplitudes of underwater spark discharges on the inductance are formalized.

Streszczenie: W artykule przedstawiono rozważania dotyczące oczyszczania odpadów galwanicznych z jonów metali ciężkich. W tym celu zastosowano elektryczne wyładowanie wieloiskrowe o rozkładzie objętościowym. Rozważano wpływ zmian indukcyjności obwodu na przebieg procesu. Główny problem naukowy dotyczy stabilizowania wyładowania w wodzie podczas trwania procesu oczyszczania. Przedstawiono wyniki w zakresie opisu zależności amplitudy i mocy podwodnych wyładowań iskrowych w funkcji indukcyjności. (Wpływ indukcyjności obwodu wyładowczego na proces oczyszczania odpadów galwanicznych metodą elektroiskrową)

Keywords: electrospark method for cleaning galvanic drains, discharge circuit inductance, electroerosive dispersion

Słowa kluczowe: metoda elektroiskrowa do czyszczenia kanałów galwanicznych, indukcyjność obwodów wyładowczych, dyspersja elektroerozyjna

Introduction

Electrical methods, such as electrospark discharge are effective methods in the different ranges of economy [1, 2] and also of wastewater treatment from heavy metals [3-6]. Volumetrically distributed multi-spark underwater discharge (VMSD) between conductive granules is a process that is effectively used to clean industrial effluents from galvanic production from heavy metal ions and other polluted waters and to obtain micron and submicron powders of metals and alloys.

Technological methods based on a volume-distributed multi-spark underwater discharge are also called volumetric electrospark dispersion of conductive granules, complex electrospark cleaning of electroplating wastes by various groups of researchers and developers.

The basic way to implement a volume-distributed multi-spark underwater discharge is as follows. A charged capacitor battery is periodically switched with a gap between two conductive surfaces-electrodes, the space between the electrodes is freely filled with conductive, most often metal granules, immersed in a weakly conductive liquid. The phenomenology of electrospark discharges at contacts between granules in a liquid, the mechanisms of spark erosion dispersion of material and electropulse cleaning of galvanic drains are studied by many researchers [7-16].

The use of a mixture of granules from different metals, for example, iron and aluminum, makes it possible to purify it from heavy metal ions (Ni^{2+} , Zn^{2+} , $\text{Cr}^{6+}+\text{Cr}^{3+}$, Cu^{2+} , $\text{Fe}(\Sigma)$) in the complex. The use of the VMSD method makes it possible to achieve the residual content of heavy metal ions by several orders of magnitude lower than that provided for by common standards [17-18].

However, to date, there are no generalized results on the conditions for stabilizing the electrical regimes of liquid processing using VMSD when using a spark load consisting of iron and aluminum granules. Stabilization here refers to the reproduction of the shape and amplitude of the discharge currents and voltages across the interelectrode gap from discharge to discharge in the charge-discharge cycle of a capacitor bank to a spark load. It is important that the spark load is not a separate conductive granule, but a

layer of granules that allows efficient processing of galvanic wastes in a flow mode. Also, the dependences of the VMSD power amplitudes on the parameters of the discharge circuit and the patterns of energy input into the interelectrode gap have not been studied. Understanding such regularities will make it possible to influence the spatial distribution of VMSD in a layer of granules, temperature conditions in plasma-erosion regions, and increase both the efficiency of cleaning galvanic wastes and the productivity of disintegration of metal granules into microcomponents. The inductance of the discharge circuit is the most important parameter that affects, among other things, the amount of energy released in the discharge channel. The amount of energy, as well as the instantaneous power of the electric discharge developed on a spark load, are factors that affect the process of electroerosion and, consequently, the efficiency of water treatment [19-20].

The aim of the research is to reveal the general patterns of changes in the electrical characteristics of volumetrically distributed multi-spark underwater discharges in a layer of metal granules depending on the inductance of the discharge circuit.

Materials and methods

The methodology of experimental studies, circuit solutions and hardware implementation of laboratory electrical equipment used in this work are described in detail in the articles [4; 17]. There is also a general description of the layout of the technological reactor for the purification of galvanic wastes using VMSD in a layer of a mixture of iron and aluminum granules. Experimental studies were carried out for a mixture of metal granules (aluminum + iron, in a mass ratio of 1:1), which is relevant from the point of view of the efficiency of cleaning galvanic waste, and the basic geometric parameters of the metal load (average characteristic granule size - 5 mm; layer of granules - 60x60x60 mm). The model liquid is tap water ($\sim 10^{-2} \text{ Ohm}\cdot\text{m}^{-1}$). The flow pattern of the liquid is vertical, from bottom to top, with a volumetric flow rate of 50 dm³/h.

Specific values of the electrical parameters of the discharge circuit and the rationale for their choice are given below in the course of presenting the results and discussing them.

Results and discussion

The capacitance of the capacitor bank (C) was fixed at a value of $40 \mu\text{F}$, the charging voltage of the storage device (U_0) was changed in the range from 150 to 600 V with an interval of 50 V. The inductance of the discharge circuit was changed by successively introducing an additional sectioned coil without a core into the discharge circuit, obtaining at this is the following series of values: 2.13; 12.77; 22.85; 34.08; 44.14; 56.46 μH .

High reproducibility from discharge to discharge of the form and levels of the time dependences of the discharge current and voltage (stable electrical processing modes) in the interelectrode gap is observed for the highest inductance of the range at $U_0 \geq 300 \text{ V}$, for the smallest - at $U_0 \geq 400 \text{ V}$ (Fig. 1).

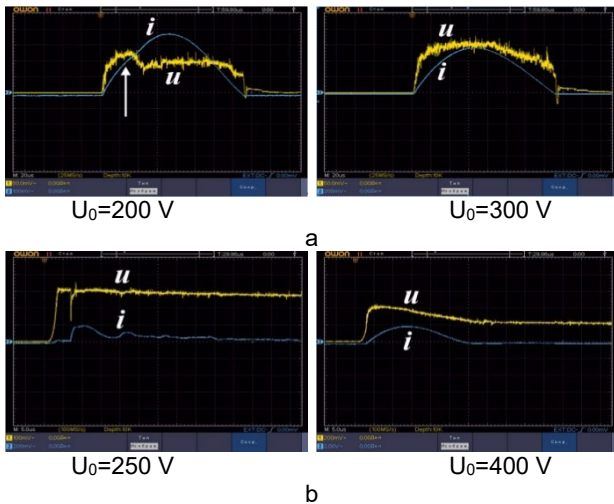


Fig. 1. Oscillograms of the discharge current (i) and voltage across the interelectrode gap (u) for $L=56.46 \mu\text{H}$ (a) and $L=2.13 \mu\text{H}$ (b) with an increase U_0 to values corresponding to the beginning of stabilization of electrical processing modes.

This result, on the whole, agrees with the data previously obtained in [20, 21]. The issue of the minimum voltage required for the formation of a spark discharge on one pair of contacts when using granules of the same conductive material was investigated [20]. A method was proposed for determining the minimum voltage for the formation of a multi-spark discharge between metal granules in layers with different geometric parameters [21].

There are some qualitative differences of electrical characteristics when changing the additional inductance L at the stage of stabilization of electrical modes. So, for $L=56.46 \mu\text{H}$, the formation of a through spark chain (or a set of parallel chains) of current flow from electrode to electrode is a longer in relation to the half-cycle of this short-circuited circuit. The closing of the interelectrode gap (IEG) by a chain of sparking contacts is manifested by a sharp decrease in the voltage drop.

For unstable electrical modes, the closure of the MEP is accompanied by an inflection of the discharge current curve (Fig. 1, a, $U_0=200 \text{ V}$), and continues with a gradual monotonous development of already formed spark chains. For $L=2.13 \mu\text{H}$, a through spark chain is rapidly formed, but after that, multiple re-formation of chains can occur during the same pulse (one switching act of the capacitor bank on the MEP) with partial degradation of the existing ones. The consequence of this effect is reusable sign-alternating kinks in the discharge current curve. This aggravated situation for unstable electrical modes can be demonstrated for the same L when using a larger capacitance of the capacitor bank, where it is more pronounced, this is qualitatively shown in Fig. 2a.

An increase in U_0 to the stabilization values for given L and C excludes such a situation (Fig. 2b), and at the same time also levels out the change from discharge to discharge in the duration of the half-cycle, the shape and amplitude of the discharge current.

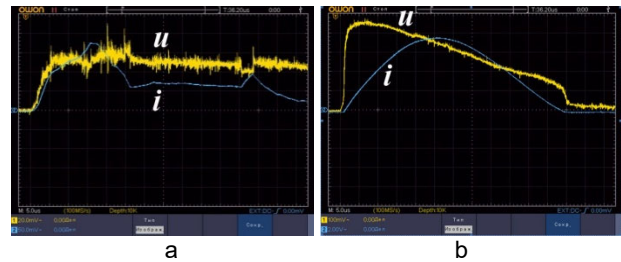


Fig. 2. Oscillograms of a prolonged spark process with a two-peak discharge current (a) and a stable electric discharge in a layer of granules (b) at the same values of L and C (the time bases are the same).

The use of other values of L within the above range does not lead to the appearance of additional features and does not affect the described nature of the change in the electrical characteristics of the VMSD.

Next, electrical processing modes are considered that are close to stable and fully stabilized, that is, those for which, with fixed C and L (var), the charging voltage of the capacitor bank is $U_0 \geq 300 \text{ V}$. As can be seen from Fig. 3, for all instantaneous powers developed on the load and calculated on the basis of oscillograms according to the formula 1.

$$(1) \quad N(t) = i(t) \cdot u(t), [\text{V} \cdot \text{A}],$$

where $i(t)$ and $u(t)$ are the time dependences of the discharge current and voltage on the MEP, depending on L for different U_0 there are some regularities.

First, the maximum values of $N(t)$ for all combinations of the studied parameters, which provide stable discharges, correspond to the post-switching moment of time::

$$(2) \quad \tau_{Nm} = \tau_{HP} / 2,5$$

where $\tau_{HP} = \pi \sqrt{L \cdot C}$ - half-period of natural oscillations of this circuit.

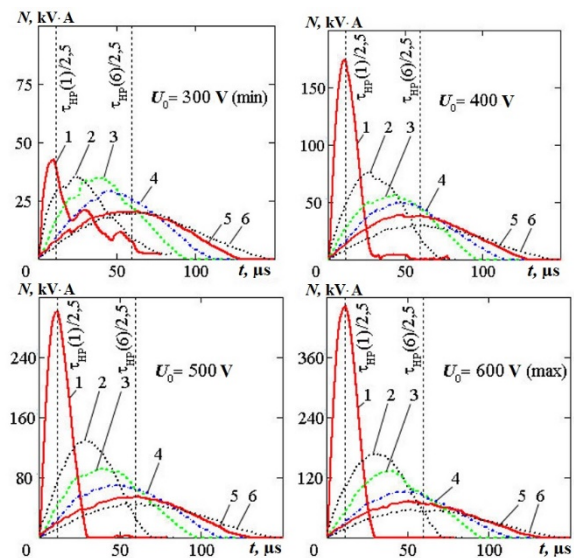


Fig. 3. Experimental dependences of the spark discharge instantaneous powers: 1 - $L=2.13 \mu\text{H}$; 2 - $L=12.77 \mu\text{H}$; 3 - $L=22.85 \mu\text{H}$; 4 - $L=34.08 \mu\text{H}$; 5 - $L=44.14 \mu\text{H}$; 6 - $L=56.46 \mu\text{H}$.

Secondly, the amplitudes of the instantaneous powers of spark discharges (N_m) for the same U_0 change almost inversely proportional to the change in $L^{0.5}$ (excluding conditions with $U_0=300$ V for $L=2.13$ μ H - but this combination of parameters still does not provide stable stabilization of electrical modes processing). This pattern of change in the amplitude of the instantaneous power is confirmed by the results of regression analysis (N_{im}) of the dependences of N_m on L for different values of U_0 (Fig. 4).

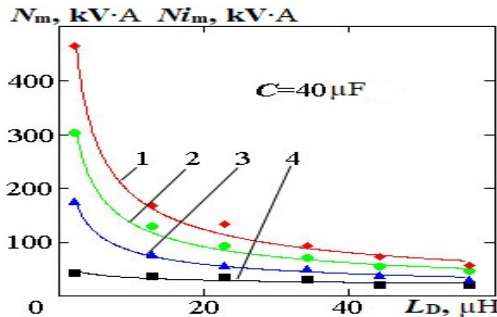


Fig. 4. Experimental values (markers, N_m) and regression dependences (solid lines, N_{im}) of spark discharge power amplitudes at different voltage values: 1 – 600 V; 2 – 500 V; 3 – 400 V; 4 – 300V.

From the analysis of the formal notation of the power regression (3) of the instantaneous power amplitudes $N_{im}(L)$, defined for L in the dimension [μ H], it follows that the ratio of the coefficients in front of L for different charging voltages is close to the ratio of the squared voltages, and the negative exponents at L are monotonically increase.

$$(3) \quad N_{im}(L) = \begin{cases} 117027 \cdot L^{-0.43}, U_0 = 300V \\ 266725 \cdot L^{-0.51}, U_0 = 400V \\ 497542 \cdot L^{-0.57}, U_0 = 500V \\ 785539 \cdot L^{-0.62}, U_0 = 600V \end{cases} \quad [V \cdot A]$$

$$(4) \quad Na_m(U_0, C, L_D) = \frac{U_0^2}{\sqrt{\frac{L_D}{C}}} \cdot e^{-\frac{\pi}{2.5}}, [V \cdot A]$$

A decrease L beyond the lower limit of the range under study in real installations is limited by technical conditions, an increase beyond the upper one is not advisable. Thus, taking into account the above time point corresponding to N_m , for all considered inductances in the basic implementation of the VMSD, we can propose formula (4) to estimate the values of N_m depending on U_0 , C and L (Fig. 5) - $Na_m(U_0, C, L)$.

The amplitude value of the power is estimated at $C=Const$, but as will be shown by our further studies, it is also valid when C changes in the range from 20 to 100 μ F. In this case, the geometric characteristics of the layer of granules are taken into account, the choice of which is justified in [16].

Relative deviations (δ_{Nm}) of the Na_m values calculated based on formula 4, from the corresponding experimental data N_m were determined based on the formula 5

$$(5) \quad \delta_{Nm} = \frac{|Na_m(U_0, C, L) - N_m(U_0, C, L)|}{N_m(U_0, C, L)} \cdot 100\%, [\%],$$

and compared with the values of the relative energy release during the discharge (η_w)

$$(6) \quad \eta_w = W_z/W_0 = \int_0^{\tau_1} i(t) \cdot u(t) dt / C \cdot U_0^2 / 2, [o.e.],$$

where W_z is the energy released on the MEP during a discharge with a duration of τ_1 , J;

W_0 is the energy stored before the discharge in the capacitor bank, J.

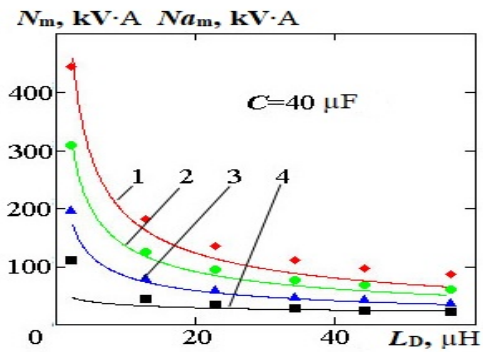


Fig. 5. Experimental dependences (solid lines, N_m) and estimated values (markers, Na_m) of spark discharge power amplitudes calculated on the basis of formula 4.

The comparison showed that for $\eta_w > 0.85$ the deviation of δ_{Nm} is several percent (maximum – 10.4%).

It is important to note that a relative energy release of more than 0.85 is optimal for the energy efficiency of the industrial application of VMSD, for example, in the treatment of galvanic drains. Thus, when $\eta_w > 0.85$, formula (4) is quite correct for its use as a formalization of the complex dependence of the electrical characteristics of the VMSD on the parameters of the discharge circuit under conditions of a fixed value of C .

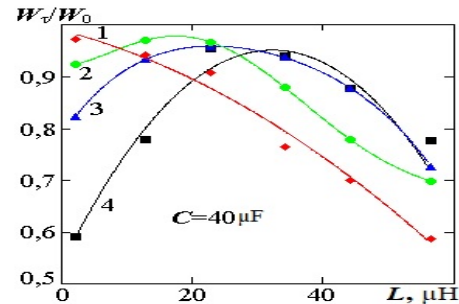


Fig. 6. Experimental dependences of the relative energy release on the interelectrode gap during the spark discharge at different voltage values: 1 – 600 V; 2 – 500 V; 3 – 400 V; 4 – 300 V.

Dependences of η_w on L (Fig. 6) are extremal, except for curve 1, in this case, apparently, the extremum corresponds to lower values than the lower limit of the investigated range of inductance values.

The inductance values at which the energy release extrema are observed for each U_0 are the conditions for matching the spark load in the discharge circuit with a capacitor bank of a certain capacity (C). Thus, these are the conditions for optimizing the parameters of the discharge circuit of electrical installations with technological action based on a volume-distributed multi-spark underwater discharge to minimize unproductive energy costs.

Conclusion

The dependences of changes in the electrical characteristics of volumetrically distributed multi-spark underwater discharges in a layer of a mixed metal load consisting of iron and aluminum granules on the inductance of the discharge circuit are revealed.

The dependences of the discharge power amplitudes on the inductance and voltage are formalized, and the estimated regularities of the input of electrical energy into the interelectrode gap are described.

The conditions for stabilizing the electrical modes of processing galvanic wastes using a volume-distributed multi-spark underwater discharge by changing the inductance of the discharge circuit are revealed.

The extrema of the energy release in the interelectrode gap to match the spark load have been determined, which will make it possible to minimize unproductive energy costs in the electrospark treatment of galvanic wastewater from heavy metal ions.

REFERENCES

- [1] Przystupa, K., & Litak, G. (2017). Electrochemical grinding of titanium-containing materials. *Advances in Science and Technology. Research Journal*, 11(4).
- [2] Przystupa, K. (2019). Electrochemical ECG grinding of ceramic and tungsten sinter. In *MATEC Web of Conferences* (Vol. 252, p. 01001). EDP Sciences.
- [3] Malyshevskaya, A., Yushchishina, A., Mitryasova, O., Pohrebennyk, V., Salamon, I. 2021. Optimization of Extraction Processes of Water-Soluble Polysaccharides under the Electric Field Action. 2021. *Przegląd Elektrotechniczny*, R. 97 NR 12, 73–76. <http://doi:10.15199/48.2021.12.12>
- [4] Petrov O., Petrichenko S., Yushchishina A., Mitryasova O., Pohrebennyk V. 2020. Electrospark Method in Galvanic Wastewater Treatment for Heavy Metal Removal. *Applied Sciences*, Special Issue «Determination and Extraction of Heavy Metals from Wastewater and Other Complex Matrices», 10(15), 5148; <https://doi.org/10.3390/app10155148>
- [5] Malyshevskaya, A., Koszelnik, P., Yushchishina, A., Mitryasova, O., Gruca-Rokosz, R. 2022. Green Approach to Intensify the Extraction Processes of Substances from Plant Materials, *Journal of Ecological Engineering*, 23(7), 197–204. <https://doi.org/10.12911/22998993/150060>
- [4] Yu, J., Yang, J., Tang, D., Dai, J. 2019 Early prediction of remaining discharge time for lithium-ion batteries considering parameter correlation between discharge stages. *Eksploracja i Niezawodność – Maintenance and Reliability*, 21(1), 81-89. <https://doi.org/10.17531/ein.2019.1.10>
- [5] Berkowitz, A.E., Hansen, M.F., Parker, F.T., Vecchio, K.S., Spada, F.E., Lavernia, E.J., Rodriguez, R. 2003. Amorphous soft magnetic particles produced by spark erosion. *Journal of Magnetism and Magnetic Materials*, 254–255, 1–6. [https://doi.org/10.1016/S0304-8853\(02\)00932-0](https://doi.org/10.1016/S0304-8853(02)00932-0).
- [6] Carrey, J., Radousky, B., Berkowitz, A. E. 2004. Spark-eroded particles: Influence of processing parameters. *J. Appl. Phys.*, 3 (95), 823-830. <https://doi.org/10.1063/1.1635973>.
- [7] Zakharchenko, S.N., Kondratenko, I.P., Perekos, A.E., Zalutsky, V.P., Kozyrsky, V.V., Lopatko, K.G. 2002. Influence of discharge pulses duration in a layer of iron granules on the sizes and structurally-phase condition of its electroerosion particles. *Eastern-European Journal of Enterprise Technologies*, 5(60), 66–72. <https://doi.org/10.15587/1729-4061.2012.5728>.
- [8] Lobanova, G., Yurmazova, T., Shiyan, L., Voyno, D. 2015. Investigation of the mechanism of microplasma impact on iron and aluminum load using solutions of organic substances. *IOP Conf. Series: Materials Science and Engineering*, 81, – URL: <http://dx.doi.org/10.1088/1757-899X/81/1/012076>
- [9] Halbedel, B., Prikhna, T., Quiroz, P., Schawohl, J., Kups, T., Monastyrov, M/ 2018 Iron oxide nanopowder synthesized by electroerosion dispersion (EED) – Properties and potential for microwave applications. *Current Applied Physics*, 18, 11. 1410-1414. <https://doi.org/10.1016/j.cap.2018.08.006>
- [10] Zakharchenko, S., Perekos, A., Shidlovska, N., Ustinov, A., Boytsov, O., Voynash, V. 2018. Electrospark Dispersion of Metal Materials. I. Influence of Velocity of Flow of Operating Fluid on Dispersion of Powders. *Metallofiz. Noveishie Tekhnol.*, 3(40), 339–357. (in Russian). DOI: 10.15407/mfint.40.03.0339.
- [11] Nguyen, P., Lee, K., Kim, S., Ahn, K., Chen, L., Lee, S., Chen, R., Jin, S., Berkowitz, A. 2012. Spark erosion: a high production rate method for producing Bi_{0.5}Sb_{1.5}Te₃ nanoparticles with enhanced thermoelectric performance. *Nanotechnology*, 23, 415604-1 – 415604-7. DOI: 10.1088/0957-4484/23/41/415604.
- [12] Liu, Y., Li, X., Li, Y., Zhao, Zh., Bai, F.: 2016. The lattice distortion of nickel particles generated by spark discharge in hydrocarbon dielectric mediums. *Applied Physics A*, 122, 174-1 – 174-9. DOI:10.1007/s00339-016-9698-2.
- [13] Malyshevskaya, A., Koszelnik, P., Yushchishina, A., Mitryasova, O., Mats, A., Gruca-Rokosz, R. 2023. Synergy Effect during Water Treatment by Electric Discharge and Chlorination, *Environments*, Special Issue "Emerging Technologies for Advanced Water Purification II", *Environments* 2023, 10(6), 93. <https://doi.org/10.3390/environments10060093>
- [14] Przystupa, K., Petrichenko, S., Mitryasova, O., Yushchishina, A., Pohrebennyk, V., Kochan, O. 2020. Electric spark method of purification of galvanic waste waters. *Przegląd Elektrotechniczny*, 96(12), (2020). 230–233. <https://doi.org/doi:10.15199/48.2020.12.50>
- [15] Malyshevskaya, A., Koszelnik, P., Yushchishina, A., Mitryasova, O., Mats, A., Gruca-Rokosz, R. 2023. Eco-Friendly Principles on the Extraction of Humic Acids Intensification from Biosubstrates, *Journal of Ecological Engineering*, 24(2), 317–327.
- [16] Shcherba, A.A., Kosenkov, V .M., Bychkov, V.M. 2015. Mathematical closed model of electric and magnetic fields in the discharge chamber of an electrohydraulic installation. *Surface Engineering and Applied Electrochemistry*, 51, 581-588. <https://doi.org/10.3103/S1068375515060113>.
- [17] Kosenkov, V.M., Bychkov, V.M. 2015. Mathematical modeling of transient processes in the discharge circuit and chamber of an electrohydraulic installation. *Surface Engineering and Applied Electrochemistry*, 51, 167–173. <https://doi.org/10.3103/S1068375515020076>.
- [18] Petrichenko, S., Kuskova, N., Listovskij, D. 2015. Comparison of the electrical characteristics of spark discharges in a layer of metal and graphite granules immersed in liquid. *Surf. Engin. Appl. Electrochem*, 3(51), 240–245. –URL: <https://doi.org/10.3103/S1068375515030138>.
- [19] Petrichenko, S., Listovskij, D., Kuskova, N. 2016. Stabilization of discharge pulses and peculiarities of matching spark load during electroerosive dispersion of metal and graphite granules in a liquid. *Surf. Engin. Appl. Electrochem*, 2(52), 134–139. – URL: <https://doi.org/10.3103/S1068375516020101>